

Ab-initio calculations for structural properties of Zr-Nb alloys

Vasyl O. Kharchenko, D. O. Kharchenko

Angaben zur Veröffentlichung / Publication details:

Kharchenko, Vasyl O., and D. O. Kharchenko. 2013. "Ab-initio calculations for structural properties of Zr-Nb alloys." *Condensed Matter Physics* 16 (1): 13801-1-13801-8.
<https://doi.org/10.5488/CMP.16.13801>.

Nutzungsbedingungen / Terms of use:

CC BY 4.0

Dieses Dokument wird unter folgenden Bedingungen zur Verfügung gestellt: / This document is made available under these conditions:
CC-BY 4.0: Creative Commons: Namensnennung
Weitere Informationen finden Sie unter: / For more information see:
<https://creativecommons.org/licenses/by/4.0/deed.de>



Ab-initio calculations for structural properties of Zr–Nb alloys

V.O. Kharchenko^{1,2}, D.O. Kharchenko¹

¹ Institute of Applied Physics of the National Academy of Sciences of Ukraine,
58 Petropavlivska St., 40030 Sumy, Ukraine

² Institute of Physics, University of Augsburg, 1 Universitätsstraße, 86135 Augsburg, Germany

Received August 27, 2012, in final form November 9, 2012

Ab-initio calculations for the structural properties of Zr–Nb alloys at different values of the niobium concentration are done at zero temperature. Different cases for Zr–Nb alloys with unit cells having BCC and HCP structures are considered. Optimal values of the lattice constants are obtained. Critical value for the niobium concentration corresponding to the structural transformation HCP → BCC at zero temperature is determined. Electronic densities of states for two different structures with niobium concentrations 12.5% and 25% having HCP and BCC structures, accordingly, are studied.

Key words: *ab-initio calculations, HCP and BCC structures, zirconium-niobium alloys*

PACS: 61.50.Lt, 61.72.Bb, 61.72.jj, 61.72.S-, 71.15.Dx, 71.15.Nc

1. Introduction

Zirconium alloys are known to be very promising materials for atomic industry and power engineering starting from the recent six decades and are of very special practical importance. Zirconium and zirconium-niobium alloys are widely used as construction materials in nuclear reactors [1–3]. The role of construction materials lies in a stability support for the whole operating period of geometry of active zones, fuel assemblies, heat-generating elements, etc. Therefore, the key problem for material science security of modern nuclear power and for the future power engineering is the study of micro-structure evolution and its effect on the behavior of physical and mechanical characteristics of material. The materials used in nuclear power engineering contain solute species in more or less dilute proportions (1% in pressure vessel steels and in cladding materials, Zr alloys). It is known that zirconium has two configurations: α -phase characterized by the HCP lattice that is stable at a low enough temperature ($< 863^\circ\text{C}$), and β -phase with BCC lattice at high temperature. Niobium has BCC lattice. Zirconium-niobium alloys characterized by α -phase are used as construction material of the active zone of nuclear reactors due to a beneficial mix of nuclear, mechanical and corrosive properties [1–3].

Alloys Zr– x Nb with a high percentage of niobium ($x > 5\%$) have a high capacity for hydrogenation which causes deterioration of corrosion properties. That is why zirconium-niobium alloys with small niobium concentration ($< 5\%$) can be advantageously used in the reactor metallurgy. In the nuclear reactor, Hydrogen diffuses inside an alloy due to corrosion processes. When the Hydrogen concentration exceeds the solubility limit, it stands out as a fragile hydride phase that limits the usage of an alloy in the reactor. Hence, the study of Zr–Nb alloys having small and high niobium concentrations, together with processes of hydride formation in zirconium-niobium alloys is an urgent problem in the novel material science. Investigations of the hydride phase formation processes in alloy Zr–Nb that contains 20% and 40% of niobium were made in [3, 4]. To study such a process in alloys having high niobium concentration, the plane strain theory was used in reference [5]. In reference [6] diffusion coefficients of Zr and Nb atoms in BCC alloys having niobium concentrations 5.5%, 16.3% and 28.1% were studied. It was found that zirconium and niobium atoms diffuse in an alloy according to the mono-vacancy mechanism.

The latter is defined by the specification of lattice dynamics. Diffusion of hafnium and niobium atoms in coarse-grained BCC alloy Zr–Nb with 19% niobium was studied in reference [7]. It was determined that diffusion coefficient of niobium is less than the hafnium one. Corrosion behavior of Zr–Nb alloy with niobium concentration variation from 0.02% to 20% was considered in [8]. It was shown that corrosion rate becomes smaller with a decrease in both bulk of the β -phase and niobium concentration in α -phase. The authors have determined that the most important factor that reduces the corrosion rate is the precipitate of the β -Nb particles and the corresponding decrease of niobium in the zirconium matrix. Experimental investigations of β -phase formation with niobium concentration of 20 ÷ 88% at irradiation were made in references [9–12]. Experimental results for the structural properties α - and β -phases in Zr–Nb alloys with variation in niobium concentration at high temperature (~ 700 K) are presented in references [13–15]. Structural properties of Zr–12.5%Nb and Zr–25%Nb were theoretically considered in [16, 17]. However, the question regarding the critical value of niobium concentration at the transition from α -phase toward β -phase (structural transformation HCP \rightarrow BCC) in zirconium-niobium alloys still remains open.

In this work, we aim to study structural properties of zirconium-niobium alloys with different niobium concentrations from the first principles at low (zero) temperature. Model structures of Zr–Nb alloys with BCC and HCP lattices will be considered. The main goal of this paper is to define optimal lattice constants of Zr–Nb alloys with BCC and HCP lattices for different niobium concentrations in the alloy. We shall define the critical value of niobium concentration that corresponds to the structural transformation HCP \rightarrow BCC. A quantitative comparison with the known experimental data will be done.

The work is organized in the following manner. In section 2, we present the models for the structures of Zr–Nb alloys and describe the research methods. In section 3, we discuss the structural properties and obtain optimal lattice constants for the structures studied. The analysis of the total energy and electronic density of states is done in section 4. We conclude in the last section.

2. Models of the structures studied and research methods

It is known that zirconium at low temperatures ($< 863^\circ\text{C}$) is characterized by β -phase (HCP structure), whereas niobium has BCC structure. Hence, it is only natural to expect that alloys Zr– x Nb will have HCP structure at low niobium concentration x whereas BCC structure will be stable for large x . Since zirconium and niobium are different only for one electron and are characterized by close package structures, one can expect that niobium atoms in the HCP zirconium lattice or zirconium atoms in the BCC niobium lattice are substitutional atoms. In reference [18] the authors have studied the super-cell of 48 atoms of HCP zirconium which has a vacancy and a niobium atom in interstitial position placed near the vacancy. It was shown that during relaxation processes, niobium atom takes a vacancy position. The latter confirms that the atoms of Zr or Nb in Zr–Nb alloys are substitutional ones.

In this paper we consider the Zr– x Nb alloys with BCC and HCP lattices where the niobium concentration x takes the values $x = 3.125\%$, 6.25% , 12.5% , 25.0% , 50.0% and $x = 75.0\%$ for both types of lattices, and additionally $x = 87.5\%$, 93.75% and $x = 96.875\%$ for BCC alloys. In such a case, structures with niobium concentrations 3.125% and 96.875% are characterized by the largest number of atoms in the unit cell, 32. Hence, for the above mentioned values of the niobium concentration x in the alloy Zr– x Nb with the unit cell of 32 atoms, a number of niobium atoms is: 1, 2, 4, 8, 16, 24, 28, 30 and 31, respectively.

Model structures of BCC alloys with 2, 16 and 30 niobium atoms in the unit cell of 32 atoms are characterized by the 221 symmetry space group; other structures have the 123 group of symmetry. All the studied structures of Zr–Nb alloys with HCP lattice are characterized by the 187 space group. The number of nonequivalent atoms of zirconium and niobium that gives a number of symmetry operations for each model of BCC and HCP structure is shown in table 1.

All calculations of structural and electronic properties for the model alloys, shown in table 1, were made within the framework of density functional theory (DFT) [19] using the linearized augmented plane wave (LAPW) method, which is implemented in software packages Wien2k [20, 21]. This method self-consistently includes basic and valence electrons and is widely used to calculate the band structure of solids [20, 21]. For all calculations, the Muffin-tin radii (R_{MT}) of both Zr and Nb were taken to be 2.1 atomic units. The basis function was expanded up to $R_{\text{MT}} \times k_{\text{max}} = 7$, where R_{MT} is the smallest radius of the muffin-tin (MT) spheres and k_{max} is the maximal value of the reciprocal lattice vectors. Wave function

Table 1. The number of niobium atoms in the unit cell of 32 atoms ($\# \text{Nb}_{\text{UC}}$) and the number of nonequivalent atoms of zirconium ($\# \text{NEA}_{\text{Zr}}$) and niobium ($\# \text{NEA}_{\text{Nb}}$) for each model structure with BCC and HCP lattices.

$\# \text{Nb}_{\text{UC}}$	Type of the lattice	$\# \text{NEA}_{\text{Zr}}$	$\# \text{NEA}_{\text{Nb}}$
1	BCC	8	1
	HCP	9	1
2	BCC	4	1
	HCP	5	1
4	BCC	3	1
	HCP	3	1
8	BCC	2	1
	HCP	2	2
16	BCC	1	1
	HCP	2	2
24	BCC	1	2
	HCP	2	2
28	BCC	1	3
	HCP	1	3
30	BCC	1	4
31	BCC	1	8

expansion inside the atomic spheres was done up to $l_{\text{max}} = 10$. Such values for k_{max} and l_{max} are standard. Deviations from these values should be considered in calculating the systems with elements having large difference in masses. Integration over the Brillouin zone was performed using 1000 k -points, which is enough for the calculation of metallic structures. The criterion for stopping the iteration process was the converge for the total energy and the charge of the crystal to less than 0.0001 Ryd and $0.001 e^-$, respectively. All calculations were made using the generalized gradient approximation (GGA) with parametrization (PBE) [22].

3. Structural relations

In this section the main results are shown for structural properties of the structures studied. The optimization procedure was used to define the optimal values of the lattice constants for each structure of Zr–Nb alloy with BCC and HCP crystals.

3.1. BCC lattice

For Zr– x Nb alloys with BCC lattice, the optimization procedure was made in the standard manner. For each value of niobium concentration x , we have defined the total energy for the unit cell of the crystal with varying in the unit cell volume. The obtained data were approximated by the equation of state [23]. The minimum on the dependence of the total energy of unit cell versus unit cell volume corresponds to the optimal value of the unit cell volume. Following the standard definition for the volume of the unit cell of the BCC-crystals $V_{\text{bcc}} = a_{\text{bcc}}^3$, the optimal value for the lattice constant a_{bcc} was determined. The dependence of the optimal lattice constant a_{bcc} on the niobium concentration x for BCC alloys Zr– x Nb is shown in figure 1.

Here, the obtained theoretical results are shown with the help of filled squares. Empty and filled triangles correspond to the experimental data (see references [24] and [13], respectively). The known value for the lattice constant of pure BCC niobium is shown by symbol \times . In figure 1 it is seen that with an increase

in the niobium concentration in the BCC Zr- x Nb alloy the lattice constant decreases according to the linear law. This result is consistent with the well known approximate empirical rule, called in metallurgy Vegard's law [25, 26]. According to this rule, at constant temperature, a linear dependence is realized between the crystal lattice parameter of an alloy and the concentrations of the constituent elements. Thus, for the studied BCC Nb $_x$ Zr $_{1-x}$ alloy, where zirconium atoms are substitutional ones in the BCC niobium lattice, the relation between lattice parameters for the pure zirconium and niobium and its alloy is given as follows: $a_{\text{ZrNb}}^{\text{bcc}} = x \cdot a_{\text{Nb}}^{\text{bcc}} + (1 - x) \cdot a_{\text{Zr}}^{\text{bcc}}$. Here, the value for the lattice constant of pure BCC niobium is known, $a_{\text{Nb}}^{\text{bcc}} = 3.3004 \text{ \AA}$, whereas $a_{\text{Zr}}^{\text{bcc}} = 3.5634 \text{ \AA}$ is a fitting parameter (at low temperatures zirconium is characterized by the HCP lattice).

It should be noted that in the interval of niobium concentration x from 10% to 50% in the BCC Zr- x Nb alloy, the experimental data slightly exceed the obtained theoretical data. This is only natural, because theoretical calculations were performed at low (zero) temperature, while the presented experimental results were obtained at evaluated temperatures [13, 24]. It was experimentally shown that in the Zr- x Nb crystal at evaluated temperatures ($\sim 700 \text{ K}$), BCC phase is realized at evaluated and large values for the niobium concentration, i.e., $\text{at.\%Nb} > 10\%$ [13, 24]. In figure 1 we also show the values for a lattice constant of BCC alloy at small niobium concentrations. In the next section we analyse the total energy values of the crystals at low (zero) temperature and define the minimal value of the niobium concentration in the alloy Zr- x Nb, where the crystal is characterized by BCC lattice.

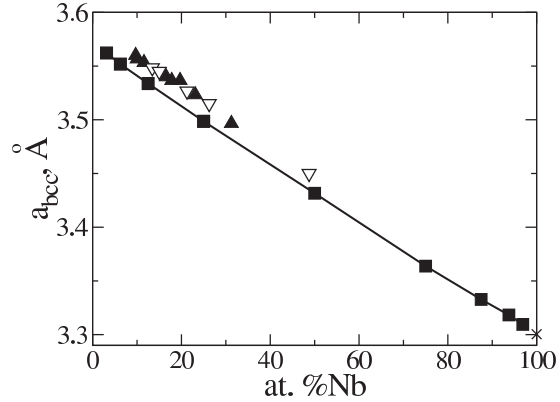


Figure 1. The dependence of the lattice parameter a_{bcc} for the BCC Zr-Nb alloys versus niobium concentration.

3.2. HCP lattice

Now, let us consider Zr- x Nb alloys with HCP lattice. The optimization procedure allowing us to find optimal lattice constants a_{hcp} and c_{hcp} for such crystals is more difficult than in the previous case for BCC lattice. This is because for the HCP alloy, one should define a global minimum of the total energy of a crystal as a function of both the volume of the unit cell and the structural relation c/a . To this end, we have proceeded in the following manner. For each value of niobium concentration, a test value of structural relation c/a was fixed. The standard optimization procedure, like in the case of BCC lattice, was used to define the optimal volume of the unit cell corresponding to the minimum of the total energy as a function of the unit cell volume, $E_{\text{min}}^{(i)}((c/a)_i)$, where $i = 1 \dots N$, N is the number of test values for the structural relation c/a . The obtained empiric data as the dependence $E_{\text{min}}(c/a)$, were approximated by the functional dependence. The minimum of this dependence corresponds to the optimal value of the structural relation $(c/a)_{\text{opt}}$ for each value of niobium concentration x in the HCP Zr- x Nb alloy. Next, for the determined $(c/a)_{\text{opt}}^{\text{Nb}}$, the standard optimization procedure was made to determine a global minimum of the total energy and the optimal unit cell volume, respectively. Using the standard definition for the volume of the HCP unit cell $V_{\text{hcp}} = (c/a)_{\text{opt}} a_{\text{hcp}}^3 \sin(2\pi/3)$ the optimal lattice constant a_{hcp} was determined for each value of the niobium concentration in the alloy. The obtained results for the lattice constant a_{hcp} and the structural relation c/a as functions on the niobium concentration x in the HCP Zr- x Nb alloy are shown in figures 2 (a) and 2 (b), respectively.

In figures 2 (a) and 2 (b), the obtained theoretical results are shown by circles. The values for the pure HCP zirconium are shown by symbol \times . First, let us consider the dependence of the lattice constant a_{hcp} versus niobium concentration shown in figure 2 (a). It is seen, that an increase in the niobium concentration x in the HCP alloy Zr- x Nb leads to a decrease in the lattice constant a_{hcp} , like in the case of the BCC crystals. However, in contrast to the previous case, the descending dependence $a_{\text{hcp}}(\text{at.\%Nb})$ differs from the linear one for the shown interval of the niobium concentration values. At low values of niobium

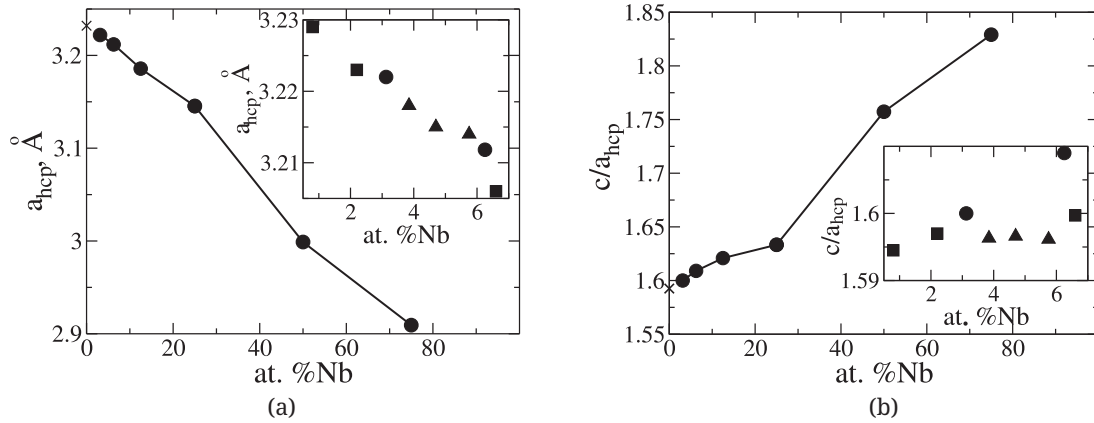


Figure 2. Dependencies of the lattice parameter a_{hcp} (a) and structural relation c/a (b) for the HCP Zr–Nb alloys versus niobium concentration.

concentrations (at.%Nb < 20%), the calculated data for the lattice constant a_{hcp} lie on the linear dependence, but for large at.%Nb, one has a deviation from the linear law. Thereby, the empiric Vegard's rule for the HCP alloys can be applied in the case of low values of niobium concentration x in Zr– x Nb alloys. In the insertion in figure 2 (a), we have shown the obtained theoretical results for a_{hcp} at low at.%Nb together with the experimental data presented by triangles and squares from [13] and [27], respectively. One can see a good quantitative correspondence with experimental results for small values of niobium concentration.

Next, let us consider the dependence of the structural relation c/a to be a function on the niobium concentration x for the HCP Zr– x Nb alloys shown in figure 2 (b). Here, the markings are made in the same way as in figure 2 (a) for the lattice constant a_{hcp} . It is seen that an increase in the niobium concentration in the alloy leads to a growth of the structural relation c/a . This means that the unit cell becomes more prolongate in z -direction. As for the lattice constant a_{hcp} , the dependence of the structural relation c/a versus niobium concentration differs from the linear law; it can be applied only for small values of at.%Nb. Comparison of the results obtained for HCP Zr–Nb alloy with experimental data from reference [13, 27] for structural relation c/a at at.%Nb < 10% shows small deviation, which is less than 1% [see insertion in figure 2 (b)].

Experimental investigations at $T \sim 700$ K indicate that HCP phase in Zr–Nb alloys is realized only if at.%Nb < 6.5% [13, 27]. Next, analyzing the values of the total energy, the maximal niobium concentration value in Zr–Nb alloy is defined, when the alloy is still characterized by HCP lattice at low (zero) temperature.

4. Total energy and electronic density of states

We have previously calculated the optimal values for lattice constants for Zr– x Nb alloys with BCC and HCP lattices at different values of niobium concentration x . Since at normal conditions pure zirconium is characterized by the HCP lattice, while pure niobium has BCC lattice, one can expect that at fixed temperature there is a critical value for niobium concentration x_c corresponding to the HCP \rightarrow BCC structural transformation. This means that for Zr– x Nb alloy at $x < x_c$, the HCP structure is energetically more favorable, whereas at $x > x_c$, the BCC structure is realized. Experimental investigations of zirconium–niobium alloys at high temperatures ($T \sim 700$ K) show that in such conditions the critical niobium concentration lies in the interval from 7 to 10% [13, 24, 27].

To define the critical value of the niobium concentration x_c at low (zero) temperature we analyze the total energies of all the crystals studied with both HCP and BCC lattices and determine the energetically most favorable structure (HCP or BCC) for each model. To this end, we proceed in the following manner. For the fixed niobium concentration x , using the obtained optimal lattice constants a_{bcc} , a_{hcp} and c_{hcp} , we perform a full cycle of *ab-initio* calculations to define the total energy for the unit cell. In our calculations

we study the unit cell containing 32 atoms: there is 1 atom of niobium and 31 atoms of zirconium for Zr-3.125%Nb and one has 31 atoms of niobium and 1 atom of zirconium for Zr-96.875%Nb. Next, we define the difference between the total energies for the unit cell of 32 atoms of HCP and BCC lattice, as:

$$\Delta E_{\text{tot}}(\text{at.\%Nb}) = E_{\text{tot}}^{\text{uc}}(\text{at.\%Nb})|_{\text{hcp}} - E_{\text{tot}}^{\text{uc}}(\text{at.\%Nb})|_{\text{bcc}}.$$

Hence, the value $\Delta E_{\text{tot}}(\text{at.\%Nb})$ defines the type of energetically most favorable lattice for the Zr- x Nb alloy at fixed value of niobium concentration x as follows: (i) if $E_{\text{tot}}^{\text{uc}}(\text{at.\%Nb})|_{\text{hcp}} < E_{\text{tot}}^{\text{uc}}(\text{at.\%Nb})|_{\text{bcc}}$, and as a result $\Delta E_{\text{tot}}(\text{at.\%Nb}) < 0$, then Zr- x Nb alloy has HCP lattice; (ii) at $E_{\text{tot}}^{\text{uc}}(\text{at.\%Nb})|_{\text{hcp}} > E_{\text{tot}}^{\text{uc}}(\text{at.\%Nb})|_{\text{bcc}}$, which yields $\Delta E_{\text{tot}}(\text{at.\%Nb}) > 0$, and the BCC lattice is realized. Therefore, the critical value of the niobium concentration x_c [or (at.\%Nb) $_c$] that defines the structural transformation HCP \rightarrow BCC at fixed temperature (low/zero temperature in the studied case) can be determined from the condition of energetic equivalence of two lattices, i.e., $\Delta E_{\text{tot}}(\text{at.\%Nb}) = 0$. The obtained results for the difference of the total energies of the unit cell of 32 atoms versus niobium concentration in Zr-Nb alloy are shown in figure 3.

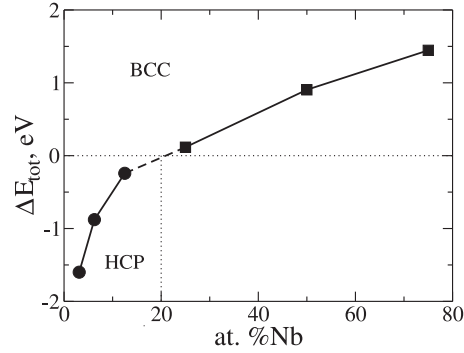


Figure 3. The difference in the total energy of HCP and BCC $\Delta E_{\text{tot}}(\text{at.\%Nb})$ structures in eV for the unit cell of 32 atoms as a function of the niobium concentration in percentage for alloys Zr-Nb.

It is seen that ΔE_{tot} changes the sign from minus to plus in the vicinity of the critical value of niobium concentration (at.\%Nb) $_c \approx 20\%$. Therefore, at low (zero) temperature, the Zr-Nb alloy with the niobium concentration less than 20% is characterized by the HCP lattice ($\Delta E_{\text{tot}} < 0$); the values for the difference ΔE_{tot} are shown by circles. In the case of large niobium concentration, i.e., over 20%, the zirconium-niobium alloy has BCC lattice (squares in the figure 3). The obtained result provides an explanation as to the deviation from the linear dependence of the obtained results for the lattice constant a_{hcp} of the HCP alloys versus niobium concentration for large at.\%Nb [see figure 2 (a)].

As was pointed out earlier, experimental investigations for the zirconium-niobium alloys at high temperatures (~ 700 K) show that the BCC phase is realized if at.\%Nb $\gtrsim 10\%$, whereas the HCP phase can be observed if at.\%Nb $\lesssim 6.5\%$ [13, 24, 27]. Thus, the theoretically obtained result from *ab-initio* calculations

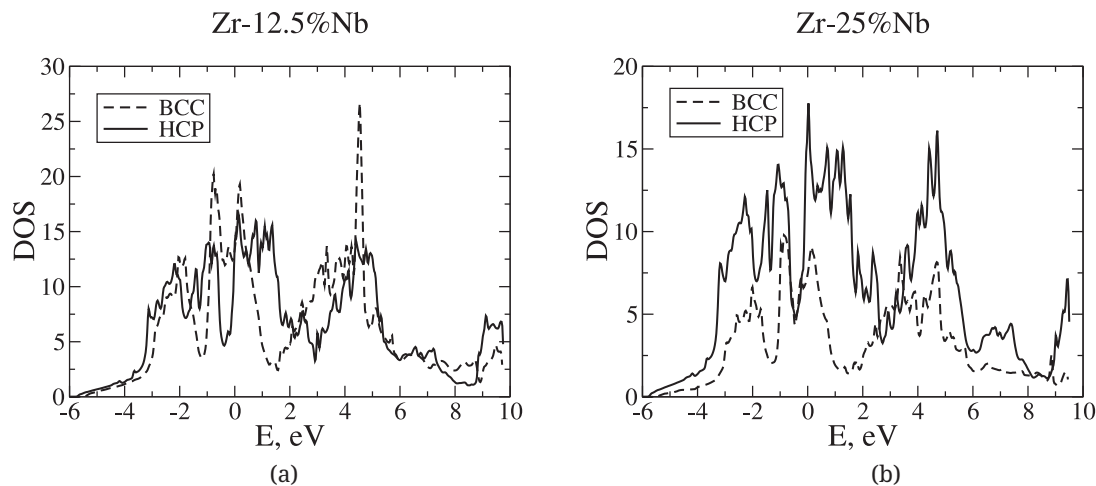


Figure 4. Dependencies for electronic densities of states (DOS) versus the energy measured from the Fermi energy for: (a) Zr-12.5%Nb alloy; (b) Zr-25%Nb alloy in the case of HCP lattice (solid curves) and BCC lattice (dashed curves).

for the critical value of niobium concentration in the Zr–Nb alloy $(\text{at.\%Nb})_c \approx 20\%$, which corresponds to the structural HCP \rightarrow BCC transformation is about twice the experimental one. An increase of the critical value of the niobium concentration with a decrease in the temperature seems to be natural. With the temperature increase, one gets thermal fluctuations becoming large in the vicinity of the lattice knots. It leads to the destruction of the more complex HCP structure at a smaller niobium concentration. Hence, one can expect a descending dependence of the critical niobium concentration $(\text{at.\%Nb})_c$ in Zr–Nb alloy versus temperature. The character of the change in the critical value $(\text{at.\%Nb})_c$ for the HCP \rightarrow BCC structural transformation with an increase in the temperature can be found using the molecular dynamics.

As far as the obtained critical niobium concentration at low (zero) temperature is $(\text{at.\%Nb})_c \approx 20\%$, next we perform calculations of the electronic density of states (DOS) for two structures: Zr–12.5%Nb and Zr–25%Nb, which are characterized by different energetically more favorable lattices, HCP and BCC, respectively. The obtained results are shown in figure 4. Here, solid curves correspond to alloys with HCP lattices, whereas dashed ones relate to alloys with BCC lattices. It is seen that for the Zr–12.5%Nb alloy the amplitude of the main peaks in the electronic density of states is larger for the BCC lattice [see figure 4 (a)], whereas for the Zr–25%Nb structure, the situation is quite different: larger DOS corresponds to the alloy with HCP lattice [see figure 4 (b)]. These results prove that at low (zero) temperature, Zr–12.5%Nb alloy is characterized by the HCP lattice, whereas alloy Zr–25%Nb has BCC lattice.

5. Conclusions

We have studied structural properties of the zirconium-niobium alloys with different niobium concentrations within the framework of *ab-initio* calculations. Niobium concentration varied from 3.125% to 96.875% for BCC and HCP lattices.

Using the optimization procedure, optimal values for the lattice constants were obtained. We have found that the introduction of zirconium atoms, as substitutional ones, into the BCC crystal of niobium leads to an increase in the lattice constant. The obtained dependence of a lattice constant versus zirconium concentration in the BCC niobium alloy is in good agreement with empiric Vegard's law and is quantitatively consistent with the known experimental data. The introduction of substitutional niobium atoms into HCP zirconium crystal causes a decrease in the lattice constant and, as a result, to an increase in the structural relation c/a . We have determined that at low (zero) temperature, the critical value of the niobium concentration in Zr–Nb alloy, which defines the structural HCP \rightarrow BCC transformation, is $(\text{at.\%Nb})_c \approx 20\%$.

References

1. Duglas D., Physical Metallurgy of Zirconium, Atomizdat, Moscow, 1975 (in Russian).
2. Dey G.K., Banerjee S., Mukhopadhyay P., J. Phys. Colloques, 1982, **43**, No. C4, 327; doi:10.1051/jphyscol:1982446.
3. Voevodin V.N., Neklyudov I.M., Structural-Phase State Evolution and Radiation Resistance of Structural Materials, Naukova Dumka, Kiev, 2006 (in Russian).
4. Dey G.K., Banerjee S., J. Nucl. Mater., 1984, **125**, 219; doi:10.1016/0022-3115(84)90547-6.
5. Srivastava D., Neogy S., Dey G.K., Banerjee S., Ranganathan S., Mater. Sci. Eng. A, 2005, **397**, 138; doi:10.1016/j.msea.2005.02.041.
6. Herzig C., Kohler U., Divinski S.V., J. Appl. Phys., 1999, **85**, 8119; doi:10.1063/1.370650.
7. Zou H., Hood G.M., Schultz R.J., Matsuura N., Roy J.A., Jackman J.A., J. Nucl. Mater., 1996, **230**, 36; doi:10.1016/0022-3115(96)00024-4.
8. Urbanic V.F., Griffiths M., ASTM Spec. Tech. Publ., 2000, **1354**, 641; doi:10.1520/STP14321S.
9. Woo O.T., McDougall G.M., Hutcheon R.M., Urbanic V.F., Griffiths M., Coleman C.E., ASTM Spec. Tech. Publ., 2000, **1354**, 709; doi:10.1520/STP14324S.
10. Cann C.D., So C.B., Styles R.C., Coleman C.E., J. Nucl. Mater., 1993, **205**, 267; doi:10.1016/0022-3115(93)90089-H.
11. Banerjee S., Vijayakar S.J., Krishnan R., J. Nucl. Mater., 1976, **62**, 229; doi:10.1016/0022-3115(76)90019-2.
12. Kim Y.S., Im K.S., Cheong Y.M., Ahn S.B., J. Nucl. Mater., 2005, **346**, 120; doi:10.1016/j.jnucmat.2005.06.004.
13. Benites G.M., Fernandez Guillermet A., Cuello G.J., Campo J., J. Alloys Comp., 2000, **299**, 183; doi:10.1016/S0925-8388(99)00683-0.
14. Benites G.M., Fernandez Guillermet A., J. Alloys Comp., 2000, **302**, 192; doi:10.1016/S0925-8388(00)00687-3.

15. Aurelio G., Fernandez Guillermet A., Cuello G.J., Campo J., J. Alloys Comp., 2002, **335**, 132; doi:10.1016/S0925-8388(01)01809-6.
16. Kharchenko V.O., Metallofiz. Noveishie Tekhnol., 2011, **33**, No. 5, 577.
17. Kharchenko V.O., Kharchenko D.O., Dvornichenko A.V., J. Nano- Electron. Phys., 2012, **4**, No. 2, 02034.
18. Xin X.K., Lai W.S., Liu B.X., J. Nucl. Mater., 2009, **393**, 197; doi:10.1016/j.jnucmat.2009.06.005.
19. Hohenberg P., Kohn W., Phys. Rev. B, 1964, **136**, 864; doi:10.1103/PhysRev.136.B864.
20. Blaha P., Schwarz K., Madsen G.K.H., Kvasnicka D., Luitz J., Computer code WIEN2K (Vienna University of Technology, 2002), improved and updated Unix version of the original [21].
21. Blaha P., Schwarz K., Sorantin P., Rickey S.B., Comput. Phys. Commun., 1990, **59**, 399; doi:10.1016/0010-4655(90)90187-6.
22. Perdew J.P., Burke K., Ernzerhof M., Phys. Rev. Lett., 1996, **77**, 3865; doi:10.1103/PhysRevLett.77.3865.
23. Murnaghan F.D., Proc. Natl. Acad. Sci. USA, 1944, **30**, 244; doi:10.1073/pnas.30.9.244.
24. Grad G.B., Pieres J.J., Fernandez Guillermet A., Cuello G.J., Granada J.R., Mayer R.E., Physica B, 1995, **213-214**, 433; doi:10.1016/0921-4526(95)00180-H.
25. Vegard L., Z. Phys., 1921, **5**, 17; doi:10.1007/BF01349680.
26. Vegard L., Z. Cryst., 1928, **67**, 239.
27. Guerillon J.P., Metaux, Corrosion, Industrie, 1972, **557**, 21.

Структурні властивості стопів Zr–Nb: моделювання з перших принципів

В.О.Харченко^{1,2}, Д.О.Харченко¹

¹ Інститут прикладної фізики НАН України, вул. Петропавлівська, 58, 40030 Суми, Україна

² Інститут фізики Аугсбургського університету, вул. Університетська, 1, 86135 Аугсбург, Німеччина

Проведено першопринципні дослідження структурних властивостей стопів Zr–Nb із довільними значеннями концентрації ніобію при нульовій температурі. Розглянуто енергетичні властивості відповідних ОЦК та ГПУ структур. Отримано оптимальні значення параметрів ґратки структур. Встановлено критичне значення концентрації ніобію у цирконій-ніобієвих стопах, що відповідає структурному перетворенню ГПУ → ОЦК. Наведено густини станів для двох структур із концентрацією ніобія 12.5% та 25%, що характеризуються ГПУ та ОЦК структурами, відповідно.

Ключові слова: першопринципні розрахунки, ГПУ та ОЦК структури, стопи цирконій-ніобій